PCCP

Accepted Manuscript

This article can be cited before page numbers have been issued, to do this please use: F. McBride and A. Hodgson, *Phys. Chem. Chem. Phys.*, 2018, DOI: 10.1039/C8CP01205A.

ROYAL SOCIETY OF CHEMISTRY

rsc.li/pccp

View Article Online
DOI: 10.1039/C8CP01205A

The reactivity of water and OH on Pt-Ni(111) films

F. McBride and A. Hodgson

The University of Liverpool, Surface Science Research Centre, Liverpool, UK

Abstract

Bimetallic Pt catalysts are of interest as water redox catalysts in low temperature fuel cells. Here we compare water and hydroxyl adsorption on Pt-Ni(111) films and a PtNi(111) alloy surface with the behaviour on the pure metals. Whereas water adsorbs and desorbs intact from close packed Pt and Ni, it dissociates on PtNi surfaces to form adsorbed hydroxyl and hydrogen. Reactivity to water increases in the order Pt(111) < monolayer Pt-Ni(111) < multilayer (2-6 ML) Pt-Ni(111) ~ PtNi(111) surface alloy and does not scale directly with the Pt strain. Hydroxyl can also be formed by reaction with pre-adsorbed O and is less stable than on pure Pt, decomposing to water and O in a broad peak near 180 K, 20 K lower than on Pt(111). The reduced stability of OH on Pt-Ni(111) films is common to all the PtNi surfaces and consistent with bimetallic PtNi surfaces showing less blocking by OH during the oxygen reduction reaction.

Introduction

Catalytic reactions of water and hydroxyl are important in reactions ranging from steam reforming to fuel cell catalysis, encouraging research to understand their interaction with metal surfaces [1, 2]. Platinum catalysts play an especial role in water redox chemistry due to their relatively low overpotential for the oxygen reduction reaction (ORR), so bimetallic Pt catalysts have been investigated extensively in order to increase the rate of the ORR and mitigate CO poisoning in low temperature fuel cells [3]. Several transition metal - Pt alloys form surface layers containing a large proportion of Pt that display enhanced oxygen reduction [3-5], with volcano type behaviour across the transition metal series as the d-band centre is depressed relative to the pure metal [6]. This enhancement is a result of the changing balance between stabilization of reactive intermediates necessary for oxygen reduction and surface blocking by inert spectator species [5]. A further advantage of alloying is to reduce the Pt loading required in a catalyst, reducing its cost and opening this system to use in less specialised applications [7].

Of the Pt alloys studied, PtNi alloys in particular show catalytic activity that is distinct from the parent surfaces [8-14]. For example, Pt_3Ni surfaces are an order of magnitude more active to the ORR than Pt [5, 15, 16], an enhancement that has been associated with a weakened interaction with blocking species, in particular OH [15]. Experimental studies on epitaxially grown Pt/Ni/Pt(111) sandwich structures [17-19] reproduce the electrochemical activity of the alloy surfaces, with theoretical simulations of $Pt_3Ni(111)$ and Pt/Ni/Pt sandwich structures relating the activity of these surfaces to the strain of the Pt

View Article Online
DOI: 10.1039/C8CP01205A

layer and the stability of intermediate species in the ORR [20-22]. Sandwich structures formed on $PtNi_3$(111) show enhanced ORR reactivity at Pt strains greater than anticipated from model calculations [23] and recently it was found that nanoparticle films of dilute Pt (20%) in Ni retain this high activity, offering the prospect of cheap, practical catalysts [24]. Since the lattice parameter of Pt is 10% greater than Ni, thin Pt films formed on Ni rich particles will be highly strained, but little is known from experiment about the chemistry occurring on such highly strained surfaces.

Here we examine water adsorption and reaction on thin Pt films and surface alloy grown on Ni(111) [25-28]. Water adsorbs intact on Pt(111) [29-32] and Ni(111) [33, 34], forming complex hydrogen bonded networks that desorb at ca. 170 K in vacuum. Dissociation does not occur, but both surfaces form hydroxyl by reaction between chemisorbed O and water. Hydroxyl formed on Pt(111) sits flat, in the atop site, forming a fully hydrogen bonded, hexagonal network with water [35, 36]. Nickel appears to behave rather differently, hydroxyl binding strongly in the hollow site and not participating in hydrogen bonding to the water layer [37, 38]. Two different types of PtNi surface are discussed here, thin films of pure Pt grown on Ni(111), referred to here as "Pt-Ni(111)" film, and a surface alloy containing both Pt and Ni in the top layer which is referred to as a "PtNi(111) alloy" surface. The term "PtNi" is used generically where both types of surface behave in the same way. We find that, unlike both the parent surfaces, Pt-Ni films and alloy surfaces react with water, dissociating it to form chemisorbed OH and H. The hydroxyl formed on PtNi film and alloy surfaces is considerably less stable than on Pt(111), decomposing just above the water desorption temperature. The chemisorbed O formed will react with water to re-form hydroxyl, with the surface tolerating considerable O loadings but remaining reactive.

Experimental

Experiments were carried out in a UHV chamber with a base pressure of 2 x 10^{-11} torr, equipped with a low current microchannel plate amplified LEED system, a quadrupole mass spectrometer (QMS) for detecting scattered or desorbed products and Pt evaporation source to deposit thin films. The Ni(111) crystal used as a substrate was mounted via Ta heating wires to liquid nitrogen cooled Ta support posts. Direct current heating allows the crystal to be heated to 1200 K and cooled to 85 K within 2-3 minutes, as described previously [33]. Sample temperature was measured by a K type thermocouple, spot welded to the edge of the crystal and was controlled by a DC heating supply. Oxygen and water are supplied via a calibrated, 2 stage molecular beam, which provides accurate gas deposition onto the front face of the sample alone. The QMS is used to measure sticking probability and determine the adsorbate coverage using the direct reflection technique [39]. The combination of molecular beam adsorption and QMS detection allows sensitive temperature programmed desorption (TPD) measurements, with no interference from adsorption on the

View Article Online
DOI: 10.1039/C8CP01205A

sample edges or support, allowing the stability and coverage of desorbing species to be compared accurately. Oxygen doses were calibrated against formation of the (2x2) Ni(111) structure. Triply distilled water, D_2O (99.9%) or $H_2{}^{18}O$ (97%) were purified by freeze thaw pumping under vacuum. The Ni(111) surface forms an intact (2√7 x 2√7)R28° water network [33], which is extremely sensitive to the long range order of the surface. TPD of water from this structure was used to confirm the quality of the Ni(111) surface and to provide a calibration of the water coverage on PtNi surfaces. Saturation of the (2√7 x 2√7)R28° structure is defined here as 1 layer of water (equivalent to 0.57 ML water relative to Ni(111), based on the structural model of Thurmer *et al.* [34]).

Pt was deposited by indirect heating of a Pt bead (Matek 99.99%) using a W heating filament in a manner used previously for Sn deposition [40, 41]. Pt films grown on Ni(111) follow a Stranski-Krastanov type mechanism, growing close to layer by layer [25-28]. LEED patterns recorded during Pt film growth match closely those reported previously by Bernard *et al.* [27] for the same Pt coverage, allowing calibration of the Pt doser against completion of the first Pt monolayer. Growth of the first Pt layer causes the Ni diffraction beams to weaken and disappear, the LEED pattern reappearing after dosing 1 layer Pt and annealing the surface to 510 K to show diffraction peaks at the Ni positions and new peaks just inside these. SXRS [25] indicates Pt covers the surface, forming a close packed layer with ~ 0.3 ML of first layer Pt pseudomorphic with Ni and the remainder showing a broad SXRS peak with an average compression of ca. 4.7%. STM images of Pt/Ni/Pt(111) and $PtNi_3$(111) surfaces also find flat Pt films and Moiré structures [17, 18, 23]. Multilayer Pt-Ni(111) films remain relatively flat, with the Pt compression decreasing only slowly with thickness, so that the average compression is still 2.5% for an 8 ML thick Pt film [25]. The variation in Pt spacing found by SXRS implies a heterogeneous Pt layer with a range of different adsorption sites available. In addition to Pt monolayer and multilayer films, a PtNi(111) alloy layer can be formed by annealing the Pt film above 673 K. This surface shows a single set of LEED diffraction beams close to the position of the Ni(111) lattice beams. The PtNi(111) alloy formed is several layers thick, with a roughly equal amount of Ni and Pt, a well defined boundary to the Ni surface and a Pt concentration that oscillates into the bulk [25, 26]. The Pt film growth and alloying behaviour observed here by LEED was consistent with that reported in the earlier studies [25-28].

View Article Online
DOI: 10.1039/C8CP01205A

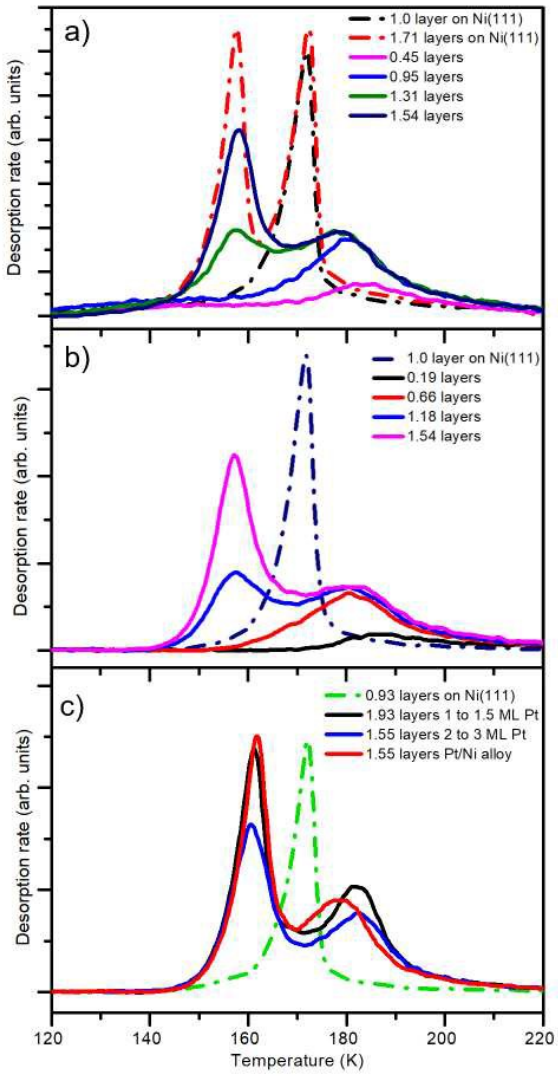

Figure 1. Desorption of water from Pt-Ni films (solid lines) compared to that from a clean Ni(111) surface (dashed lines). (a) shows desorption from a Pt monolayer on Ni(111) as a function of water dose, and (b) from a Pt multilayer (2-3 layers). (c) comparison of water desorption from the Pt monolayer, 2-3 layer Pt and PtNi(111) alloy surfaces. The heating rate was 0.8 Ks^{-1}.

Results

Adsorption-desorption experiments were performed on the Pt-Ni(111) films and PtNi(111) alloy surface to investigate the binding energy of water and compare its reactivity to that of Pt(111) and Ni(111) surfaces. Both H_2O, D_2O and $H_2{}^{18}O$ were deposited, but no differences were found between the desorption characteristics or reactivity of the different isotopes. Figure 1 compares water TPD from Ni(111) (dotted lines) with that from Pt films of different thickness and a PtNi(111) surface alloy. Water desorbs from Ni(111) in a well defined first layer peak near 170 K, with a multilayer peak forming above 150 K as the coverage is increased further. The adsorption-desorption

View Article Online
DOI: 10.1039/C8CP01205A

behaviour of water on Ni(111) is almost identical to that of Pt(111) (not shown here, see references [29, 30]), both surfaces forming intact water networks with a desorption peak at *ca.* 170 K, reflecting the similar binding energy (53.6 kJ/mol on Ni(111) [38] versus 51.3 kJ/mol on Pt(111) [42] at 0.5 ML coverage). Water desorption from Pt-Ni(111) film and PtNi(111) alloy surfaces differs from that of either parent surface, Fig. 1. At low water coverage a broad TPD peak appears between 180 and 220 K, growing into a peak near 180 K as the coverage is increased. This peak is stabilised by *ca.* 10 K compared to desorption from Ni(111) and has a long tail extending to ca. 220 K, something that is not observed for either of the plane surfaces. The 180 K peak saturates with increasing coverage and is followed by formation of a second peak near 150 K, which does not saturate and is associated with the water multilayer. Integrating the desorption peaks shows that the amount of water desorbing in the monolayer TPD peak from the single layer Pt film (Fig. 1a) is just 75-80% that from the water monolayer on Ni(111), but the width of the peak is over three times greater than its Ni(111) counterpart. Increasing the thickness of the Pt film to 2-3 ML has little effect on the peak desorption temperature, Fig. 1b, but the peak broadens slightly compared to the monolayer Pt film and the water desorption yield reduces further, with the first layer desorption peak containing approximately 60% the amount of water present in the first layer on Ni(111). Increasing the Pt film thickness to 4-6 layers Pt caused no significant change in the water TPD profiles. Desorption from the PtNi(111) alloy surface, formed by annealing a Pt overlayer to 673 K, is compared to the two Pt films in Fig. 1c. The first layer peak appears slightly below 180 K in this case, but again the water desorption peak is broad and extends above 200 K with a similar yield of water to that found from the multilayer (2-6 layer) Pt film.

Apart from the increased peak desorption temperature, the kinetics of water desorption from the Pt film and alloy surfaces are different from the parent surfaces. Water desorption from Ni(111) [33] and Pt(111) [29, 30] are zero order, the desorption traces for different water coverage all sharing the same leading edge. This behaviour can be attributed to an indirect desorption process, where dense hydrogen bonded water islands populate a dilute, weakly bound molecular state that acts as a precursor to desorption. In contrast the water desorption traces from Pt films on Ni(111) show a steady decrease in peak position with increasing coverage. TPD traces for different water coverage share a common trailing edge, something that typically arises by one of two possible mechanisms. The first is the presence of adsorption sites with different binding energies, with the less stable sites being filled sequentially only as the water coverage is increased. This behaviour would be consistent with an inhomogeneous Pt film that has a range of binding sites, reflecting the variation in Pt spacing within the film found by SXRD [25]. An alternative mechanism is second order desorption kinetics with a constant binding energy, for example caused by water (partial) dissociation followed by OH recombination to form water during heating.

View Article Online
DOI: 10.1039/C8CP01205A

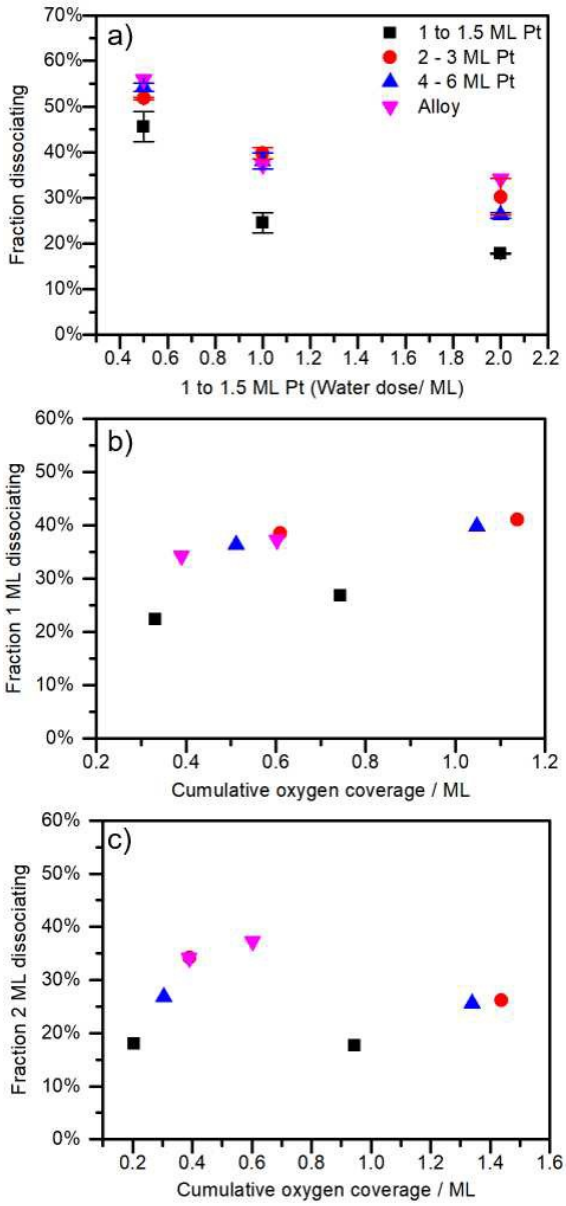

Fig. 2. Water dissociation probability determined from comparison of the water uptake with the desorption yield for different water doses. a) shows the probability of irreversible adsorption during a sequence of water (D_2O) adsorption-desorption cycles on four different PtNi surfaces, monolayer Pt, 2-3 ML Pt, 4-6 ML Pt and the PtNi(111) alloy surface. The error limits represent the full range of 2 or 3 measurements on freshly prepared surfaces. In b) and c) the dissociation probability is plotted for a fixed water dose (1 or 2 layers of water respectively) against the cumulative coverage of O present at the end of each adsorption cycle.

Since the desorption temperature of water from the PtNi surfaces is higher than that found for intact adsorption on other metal surfaces [43], we must consider whether water adsorbs and desorbs intact or if it is dissociated to form OH or O. Comparing the amount of water adsorbed from the beam with that desorbed during the subsequent TPD allows us to determine if any water is irreversibly

View Article Online
DOI: 10.1039/C8CP01205A

adsorbed on the surface. The adsorption and desorption measurements were calibrated against the corresponding signals for water adsorption-desorption on bare Ni(111), where water remains intact [33]. Figure 2a shows the fraction of water that remains on the surface as a function of the water dose during sequences of repeated D_2O adsorption-desorption on different PtNi films. We find a substantial fraction of the water is irreversibly adsorbed, remaining on the surface after water desorption is complete at ca. 220 K, implying water has dissociated. Multilayer Pt films (2-3 and 4-6 layers Pt) and the PtNi(111) alloy surface have similar dissociation probabilities, but dissociation is noticeably less efficient on the Pt monolayer (solid squares, Fig. 2). Deposition of 0.5 layer of water on a Pt multilayer film results in around half the water dissociating, with the dissociation probability dropping only slightly for deposition of 1 and 2 layers of water. In a single adsorption–desorption cycle depositing 3 layers of water (1.71 ML water relative to Ni), ~ 0.4 ML of O atoms are deposited on the surface. The data shown in Fig. 2(a) includes measurements that already have O present on the surface from previous water adsorption-desorption cycles, but the presence of chemisorbed O has remarkably little effect on the dissociation probability of subsequent water layers. Figure 2b,c show the dissociation probability plotted against the amount of O that remains on the surface after each water TPD. Continued water exposure eventually inhibits dissociation, but the PtNi surfaces are able to accommodate several monolayers of O while remaining reactive to water.

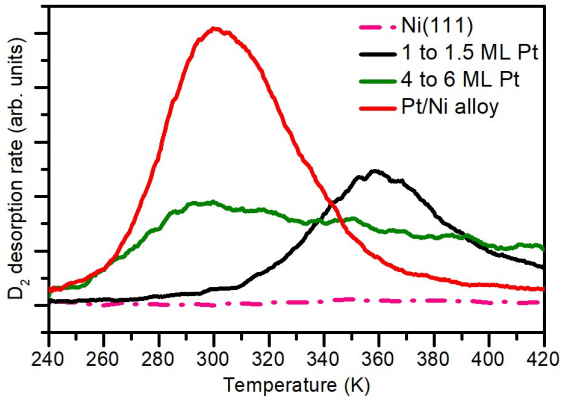

Figure 3. D_2 TPD peaks evolved during dissociation of D_2O on three different PtNi surfaces. The dashed line shows no D_2 is formed as D_2O adsorbs and desorbs intact from Ni(111). The heating rate for D_2O TPD (0.8 Ks^{-1}) was increased to 1.5 Ks^{-1} at 240 K to monitor D_2 TPD and the ramp suspended at 420 K to avoid further annealing the surface and changing the surface structure.

To confirm that D_2O dissociates we used TPD to look for formation of chemisorbed D during water desorption, shown in Fig. 3. As expected, water adsorbs and desorbs intact from Ni(111) and no D is present on the surface. All the PtNi surfaces studied here evolve D_2, confirming water dissociation occurs to form chemisorbed D on the surface. The TPD traces were limited to 420 K to prevent

View Article Online
DOI: 10.1039/C8CP01205A

further thermal evolution of the Pt film, so recombination is only partially complete when the temperature ramp is suspended and the D_2 yield cannot be used to confirm the degree of dissociation. The recombination kinetics are noticeably different between the PtNi(111) alloy surface and the Pt-Ni(111) films, with D_2 evolution occurring at a lower temperature on the alloy surface than from either the Pt-Ni(111) films or from Pt(111) [44]. The long high temperature tail to the D_2 TPD profiles from the Pt-Ni(111) films suggests D has a range of high binding energy sites in the Pt films and kinetics that are significantly different from those on the PtNi(111) alloy surface.

No further water is evolved from the PtNi surfaces above 220 K, indicating that OH has decomposed and only chemisorbed O remains on the surface. Dosing PtNi surfaces with O, followed by water, results in TPD traces that are very similar to those obtained for pure water. Figure 4 shows the effect of O adsorption prior to adsorbing water on a monolayer Pt-Ni(111) surface. Although the leading edge differs slightly, reflecting the kinetics of reaction to produce the hydroxyl phase (either water dissociation or reaction with O, depending on the initial O coverage), the same broad peak forms near 180 K as appears during desorption from a bare PtNi surface. The two different preparation routes lead to identical desorption rates above 180 K, supporting the idea that the phases formed are similar. In order to confirm that chemisorbed O reacts with water, rather than simply stabilising it by H-bonding (as occurs at high coverage of O on surfaces such as Ru(0001) [45, 46]), we performed $^{16}O + H_2{}^{18}O$ isotope exchange experiments on the PtNi surfaces. Different coverages of ^{16}O were adsorbed onto the surface and then $H_2{}^{18}O$ water was deposited from the molecular beam. $H_2{}^{18}O$ and $H_2{}^{16}O$ desorption was monitored on mass peaks 20, 18 and 17 using the TPD of $H_2{}^{18}O$ and $H_2{}^{16}O$ from the clean Ni(111) surface was used to establish the degree of ^{18}O exchange with water on the chamber walls and the cracking pattern of $H_2{}^{16}O$, allowing the mass 18 or 17 signals to be corrected to provide desorption yields. The resulting TPD traces show $H_2{}^{18}O$ and $H_2{}^{16}O$ desorbing statistically, confirming that chemisorbed O exchanges freely with adsorbed water via formation of OH. We conclude that the broad water TPD peak near 180 K on Pt-Ni(111) films and the PtNi(111) alloy surface originates from an OH or mixed OH/H_2O phase that can be formed directly by dissociation of water or by reaction with chemisorbed O.

View Article Online
DOI: 10.1039/C8CP01205A

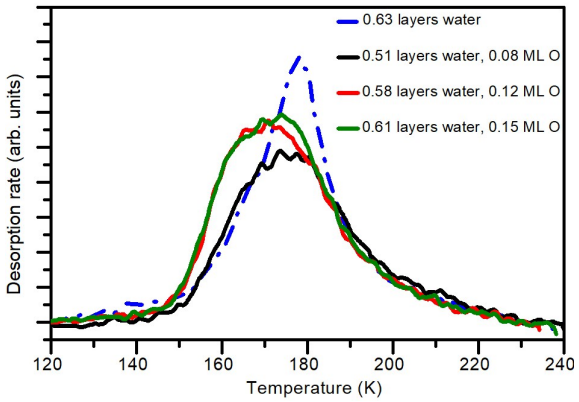

Figure 4. Water TPD traces showing the effect of pre-dosed oxygen (0.08 to 0.15 ML) on water desorption from a Pt monolayer on Ni(111). The dashed line shows water TPD from a bare Pt monolayer surface and the solid lines that for different O coverage. The exposure of water was kept constant, equivalent to one layer on clean Ni(111). The heating rate was 0.8 Ks^{-1}.

Discussion

Water adsorbed on thin (1 to 6 ML) films of Pt on Ni(111) and a PtNi(111) surface alloy dissociates efficiently to form OH and then O, with H recombining to form H_2 above 280 K, without reacting with the chemisorbed O. This behaviour is unlike that of the parent metal surfaces, which are inert, adsorbing and desorbing water intact even from low coordination step sites [47]. The OH phase formed has an unusually low decomposition temperature, desorbing near 180 K, some 20 K lower than that found for OH/H_2O decomposition on unstrained Pt(111) [36] and 10 K below that on Pd(111) [48]. There has been disagreement if water reacts with O on Ni(111) to form OH, but recent EELS [37] and calorimetry measurements [38] indicate OH is formed at low O coverage. This phase decomposes in a broad peak with a maxima around 210 K in our measurements on pure Ni(111), similar to the temperature reported earlier [49-51]. Water will also dissociate spontaneously on more reactive transition metal surfaces, such as Ru(0001) [52], but again the OH phase only decomposes to water and O near 210 K, similar to the temperature on Pt(111) and considerably higher than seen on the PtNi surfaces. These reactive metal surfaces rapidly become passivated by chemisorbed O even at low coverage (>0.09 ML O [52]), O instead forming H-bonds to water [45, 46]. In contrast, PtNi surfaces remain reactive even when covered by several monolayers of O, Fig. 2. The mechanism for this is unclear, but suggests that the Ni may accommodate a considerable O loading before the Pt film becomes passivated. The combination of reactivity towards water, facile reaction between adsorbed O and water and low decomposition temperature for OH observed on the PtNi surfaces is unlike that seen on other metal surfaces [43].

Several theoretical studies have examined the stability of oxygen reduction intermediates on Pt_3Ni

View Article Online
DOI: 10.1039/C8CP01205A

alloy and Pt-alloy surfaces, correlating the Pt strain and *d* band suppression to the stability of OH and the ORR activity [7, 20-22]. These studies provide insight into the variation in barrier height for different steps in the ORR process and predict an increase in activity up to ~ -2% strain, followed by a decrease at higher strain [7]. The 10% lattice mismatch between Pt and Ni causes a particularly large compressive stress for thin Pt films on bulk Ni(111), with an average compression of ~4.7% for monolayer Pt, dropping to ~2.5% for an 8 ML thick Pt film [25]. Our experiments indicate the reactivity of PtNi surfaces to water does not correlate directly to the degree of strain in the Pt film, which would predict decreasing reactivity at such high strain. Although monolayer Pt shows the greatest compression compared to bulk Pt, it is slightly less reactive than Pt multilayers (2-6 layers), or the PtNi(111) surface alloy. In addition, despite their very different compositions, the Pt-Ni(111) films and the surface alloy show very similar OH decomposition behaviour, irrespective of film thickness, indicating the stability of OH is not determined solely by the Pt strain, or the *d* band position as modelled by DFT. Deviation from the simple strain model has previously been observed for the ORR activity on highly strained $PtNi_3$(111) [23] and PtCu nanoparticles [53], with strains estimated as *ca.* -3% and > -4% respectively, with the ORR reactivity continuing to increase at higher strain than was anticipated by calculations [7]. The unusual combination of reactivity found on PtNi is presumably associated with the combined influence of the modified electronic structure of Pt on Ni [20-22] and the presence of a range of different Pt reaction sites in close proximity on the highly strained, inhomogeneous PtNi surface. Whereas the existing DFT models of bimetallic Pt surfaces typically assume a simple commensurate Pt film, STM studies on $PtNi_3$(111) [23] reveal the formation of Moiré structures as the Pt changes registry to the underlying Ni, supporting the idea that surface sites may have a very different local environment and reactivity to that modelled in slab calculations. The enhanced activity of these highly strained Pt films over those calculated by DFT indicates the local Pt structure plays a role in determining the surface activity and needs to be considered explicitly during modelling. Nevertheless, the insensitivity of reaction to the precise details of the PtNi surface grown offers encouragement that the catalytic response of this system may be robust in practical use [17, 24].

Conclusions

Unlike the unreactive parent metals, thin Pt and alloy layers on Ni(111) dissociate water to form hydroxyl and chemisorbed H. The hydroxyl formed decomposes near 180 K with a long tail towards 220 K, indicative of a range of binding sites on the PtNi surface, and is insensitive to the thickness of the Pt film. Chemisorbed O can build up to more than monolayer total coverage, but remains reactive, exchanging O with coadsorbed water. This combination of reactivity towards water, facile OH decomposition and reaction with water are of interest in understanding the practical activity of these films in redox catalysis.

View Article Online
DOI: 10.1039/C8CP01205A

References

1. M. H. Shao, Q. W. Chang, J. P. Dodelet and R. Chenitz, *Chemical Reviews*, 2016, **116**, 3594-3657.
2. Z. W. Seh, J. Kibsgaard, C. F. Dickens, I. B. Chorkendorff, J. K. Norskov and T. F. Jaramillo, *Science*, 2017, **355**, eaad4998.
3. M. Escudero-Escribano, P. Malacrida, M. H. Hansen, U. G. Vej-Hansen, A. Velazquez-Palenzuela, V. Tripkovic, J. Schiotz, J. Rossmeisl, I. E. L. Stephens and I. Chorkendorff, *Science*, 2016, **352**, 73-76.
4. J. Greeley, I. E. L. Stephens, A. S. Bondarenko, T. P. Johansson, H. A. Hansen, T. F. Jaramillo, J. Rossmeisl, I. Chorkendorff and J. K. Norskov, *Nature Chemistry*, 2009, **1**, 552.
5. V. R. Stamenkovic, B. S. Mun, M. Arenz, K. J. J. Mayrhofer, C. A. Lucas, G. F. Wang, P. N. Ross and N. M. Markovic, *Nature Materials*, 2007, **6**, 241-247.
6. V. Viswanathan, H. A. Hansen, J. Rossmeisl and J. K. Norskov, *Acs Catalysis*, 2012, **2**, 1654-1660.
7. I. E. L. Stephens, A. S. Bondarenko, U. Gronbjerg, J. Rossmeisl and I. Chorkendorff, *Energy & Environmental Science*, 2012, **5**, 6744-6762.
8. H. H. Hwu, J. Eng and J. G. G. Chen, *Journal of the American Chemical Society*, 2002, **124**, 702-709.
9. J. R. Kitchin, N. A. Khan, M. A. Barteau, J. G. Chen, B. Yakshinksiy and T. E. Madey, *Surface Science*, 2003, **544**, 295-308.
10. O. Skoplyak, M. A. Barteau and J. G. G. Chen, *Journal of Physical Chemistry B*, 2006, **110**, 1686-1694.
11. J. G. Chen, C. A. Menning and M. B. Zellner, *Surface Science Reports*, 2008, **63**, 201-254.
12. M. D. Skoglund, C. L. Jackson, K. J. McKim, H. J. Olson, S. Sabirzyanov and J. H. Holles, *Applied Catalysis a-General*, 2013, **467**, 355-362.
13. A. R. Morris, M. D. Skoglund and J. H. Holles, *Applied Catalysis a-General*, 2015, **489**, 98-110.
14. C. Zhang, Q. H. Lai and J. H. Holles, *Catalysis Science & Technology*, 2016, **6**, 4632-4643.
15. V. R. Stamenkovic, B. Fowler, B. S. Mun, G. F. Wang, P. N. Ross, C. A. Lucas and N. M. Markovic, *Science*, 2007, **315**, 493-497.
16. V. R. Stamenkovic, B. S. Mun, K. J. J. Mayrhofer, P. N. Ross and N. M. Markovic, *Journal of the American Chemical Society*, 2006, **128**, 8813-8819.
17. N. Todoroki, T. Dasai, Y. Asakimori and T. Wadayama, *Journal of Electroanalytical Chemistry*, 2014, **724**, 15-20.
18. N. Todoroki, Y. Asakimori and T. Wadayama, *Physical Chemistry Chemical Physics*, 2013, **15**, 17771-17774.
19. T. Wadayama, N. Todoroki, Y. Yamada, T. Sugawara, K. Miyamoto and Y. Iijama, *Electrochemistry Communications*, 2010, **12**, 1112-1115.
20. V. Viswanathan, H. A. Hansen, J. Rossmeisl, T. F. Jaramillo, H. Pitsch and J. K. Norskov, *Journal of Physical Chemistry C*, 2012, **116**, 4698-4704.
21. Y. Sha, T. H. Yu, B. V. Merinov, P. Shirvanian and W. A. Goddard, *Journal of Physical Chemistry C*, 2012, **116**, 21334-21342.
22. W. J. Xu, D. J. Cheng, M. Niu, X. H. Shao and W. C. Wang, *Electrochimica Acta*, 2012, **76**, 440-445.
23. M. Asano, R. Kawamura, R. Sasakawa, N. Todoroki and T. Wadayama, *Acs Catalysis*, 2016, **6**, 5285-5289.
24. N. Todoroki, T. Kato, T. Hayashi, S. Takahashi and T. Wadayama, *Acs Catalysis*, 2015, **5**, 2209-2212.
25. O. Robach, H. Isern, P. Steadman, K. F. Peters, C. Quiros and S. Ferrer, *Physical Review B*, 2003, **68**, 214416.
26. S. Deckers, S. Offerhaus, F. Habraken and W. F. Vanderweg, *Surface Science*, 1990, **237**, 203-212.

View Article Online
DOI: 10.1039/C8CP01205A

27. J. A. Barnard and J. J. Ehrhardt, *J. Vac. Sci. Technol. A-Vac. Surf. Films*, 1990, **8**, 4061-4068.
28. J. A. Barnard, J. J. Ehrhardt, H. Azzouzi and M. Alnot, *Surface Science*, 1989, **211-212**, 740-748.
29. S. Haq, J. Harnett and A. Hodgson, *Surface Science*, 2002, **505**, 171-182.
30. J. L. Daschbach, B. M. Peden, R. S. Smith and B. D. Kay, *Journal of Chemical Physics,* 2004, **120**, 1516-1523.
31. G. Zimbitas and A. Hodgson, *Chemical Physics Letters*, 2006, **417**, 1-5.
32. S. Nie, P. J. Feibelman, N. C. Bartelt and K. Thurmer, *Physical Review Letters*, 2010, **105**, 026102.
33. M. E. Gallagher, S. Haq, A. Omer and A. Hodgson, *Surface Science*, 2007, **601**, 268-273.
34. K. Thurmer, S. Nie, P. J. Feibelman and N. C. Bartelt, *Journal of Chemical Physics,* 2014, **141**, 18C520.
35. G. S. Karlberg and G. Wahnstrom, *Journal of Chemical Physics*, 2005, **122**, 194705.
36. C. Clay, S. Haq and A. Hodgson, *Physical Review Letters*, 2004, **92**, 046102.
37. J. Shan, A. W. Kleyn and L. B. F. Juurlink, *Chemphyschem*, 2009, **10**, 270-275.
38. W. Zhao, S. Carey, Z. Mao and C. T. Campbell, *ACS Cat.*, 2018, **8**, 1485-1489.
39. D. A. King and M. G. Wells, *Surface Science*, 1972, **29**, 454-482.
40. A. Massey, F. McBride, G. R. Darling, M. Nakamura and A. Hodgson, *Physical Chemistry Chemical Physics*, 2014, **16**, 24018-24025.
41. F. McBride, G. R. Darling, K. Pussi and A. Hodgson, *Physical Review Letters*, 2011, **106**, 226101.
42. W. D. Lew, M. C. Crowe, E. Karp and C. T. Campbell, *Journal of Physical Chemistry C*, 2011, **115**, 9164-9170.
43. A. Hodgson and S. Haq, *Surface Science Reports*, 2009, **64**, 381-451.
44. K. Christmann, G. Ertl and T. Pignet, *Surface Science*, 1976, **54**, 365-392.
45. A. Shavorskiy, M. J. Gladys and G. Held, *Physical Chemistry Chemical Physics*, 2008, **10**, 6150-6159.
46. A. Mugarza, T. K. Shimizu, P. Cabrera-Sanfelix, D. Sanchez-Portal, A. Arnau and M. Salmeron, *Journal of Physical Chemistry C*, 2008, **112**, 14052-14057.
47. M. van der Niet, O. T. Berg, L. B. F. Juurlink and M. T. M. Koper, *Journal of Physical Chemistry C*, 2010, **114**, 18953-18960.
48. C. Clay, L. Cummings and A. Hodgson, *Surface Science*, 2007, **601**, 562-568.
49. M. Schulze, R. Reissner, K. Bolwin and W. Kuch, *Fresenius Journal Of Analytical Chemistry*, 1995, **353**, 661-665.
50. T. E. Madey and F. P. Netzer, *Surface Science*, 1982, **117**, 549-560.
51. T. Pache, H. P. Steinruck, W. Huber and D. Menzel, *Surface Science*, 1989, **224**, 195-214.
52. C. Clay, S. Haq and A. Hodgson, *Chemical Physics Letters*, 2004, **388**, 89-93.
53. P. Strasser, S. Koh, T. Anniyev, J. Greeley, K. More, C. Yu, Z. Liu, S. Kaya, D. Nordlund, H. Ogasawara, M. F. Toney and A. Nilsson, *Nature Chemistry*, 2010, **2**, 454-460.

View Article Online
DOI: 10.1039/C8CP01205A

TOC graphic

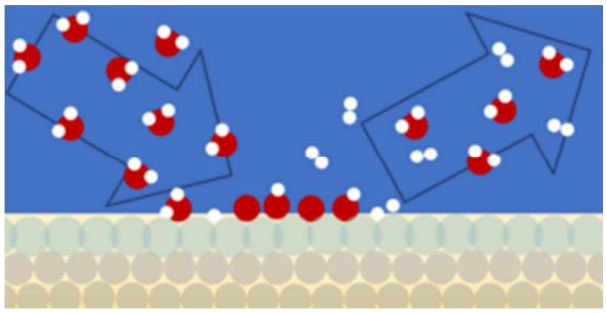

Highly strained Pt-Ni(111) films display quite different reactivity to their parent surfaces, dissociating water efficiently but not being passivated by oxygen or hydroxyl.